2012 IEEE/RSJ International Conference on
Intelligent Robots and Systems
October 7-12, 2012. Vilamoura, Algarve, Portugal

# Steady Spiraling Motion of Gliding Robotic Fish

Feitian Zhang, Fumin Zhang and Xiaobo Tan

*Abstract*— **A gliding robotic fish is developed for promising applications in aquatic environment monitoring. The design concept combines the strengths of both underwater gliders and robotic fish, featuring long operation duration and high maneuverability. This paper presents both analytical and experimental results for the three-dimension spiraling motion, an essential working pattern of the gliding fish for detecting pollution in a water column. A dynamic model of the gliding robotic fish with actuated tail is established. Then the steady-state spiraling equations are derived and solved recursively using Newton's method. The gliding fish prototype is tested in experiments. Both model prediction and experimental results show that the spiraling motion has very low energy consumption, and the gliding fish can achieve high maneuverability with a turning radius less than 1 m, 2.5% of the reported turning radius of a typical underwater glider.**

## I. Introduction

Aquatic environmental protection is a key challenge for sustainable development worldwide. Autonomous underwater robots are being widely used in this domain to patrol seaports, track oil spills, and monitor harmful algal blooms. High energy-efficiency and high maneuverability are desired characteristics for the robots in order to operate in versatile environments such as lakes, rivers, and the ocean. Underwater gliders, which propel themselves by changing net buoyancy and center of gravity, have demonstrated low power consumption and long operating duration. After two decades of development, gliders are now commercially available, examples of which include the Seaglider [1], the Spray [2] and the Slocum [3]. These gliders are designed for ocean sampling purposes with typical length within 1-2 meters, weight at 50 kg and above. Their maneuverability is not designed to operate in environments such as rivers and shallow lakes. A different class of aquatic robots that mimic fish motion has been developed in parallel to the gliders over the past two decades. These robots, often called robotic fish, can swim by deforming the body and fish-like appendages [4]–[10]. Like their biological counterparts, robotic fish are highly maneuverable in a broad range of environments.

We have developed a gliding robotic fish. Our design aims to combine features from an underwater glider and a robotic fish [11] to offer maneuverability and endurance at the same time. Locomotion of the gliding robotic fish is generated mostly by controlling the net buoyancy, and changing the center of mass, similar to an underwater glider. On the other hand, steering is mostly achieved by actively controlled fins, similar to a robotic fish. In addition, the gliding robotic fish is designed to have much smaller size than an commercial underwater glider. With appropriate sensing capability developed, we expect the gliding fish to be suitable for locating pollutants in shallow water for an extended period of time, e.g., weeks or even months.

This paper presents theoretical and experimental results on designing a three dimensional motion pattern for the gliding robotics fish to sample a water column. A water column is a conceptual narrow volume (like a narrow cylinder) of water stretching vertically from the surface to the bottom. Water column sampling is a routine surveying method in environmental studies to evaluate the stratification or mixing of water layers [12]. Aquatic pollution detection inside a water column with approximately one meter radius is frequently performed for environmental monitoring in shallow water. Existing approach for water column sampling relies on humans to operate the boat and to deploy sensing packages on the spot, which is labor-intensive and costly. We propose an autonomous solution based on the spiraling motion that can be performed by the gliding robotic fish with low-energy consumption. Spiraling motion have been observed for underwater gliders, which is typically enabled translational and rotational displacement of an internal movable mass [13]–[16]. So far, the spiraling motion produced by underwater gliders have typical turning radius on the order of 30-50 meters, not suitable for the water column sampling tasks in lakes and shallow areas. The spiraling motion produced by our gliding fish, on the other hand, can achieve the desired turning radius of less than one meter, due to the overall smaller dimensions and the controllable moment generated by the tail.

Following the theoretical approach established in the literature on analyzing the dynamics of underwater gliders [13]–[16], we first derive the three-dimension steady-state equations for the gliding fish from the dynamics model. The major extension of our model from the existing glider models is the incorporation of an actuated tail, which results in different sets of steady equilibrium motion from those of an underwater glider. We have also employed Newton's method to compute the equilibrium motion, which gives reliable convergence. The influences of various control inputs on the spiraling performance, such as turning radius and descending speed, are computed. Furthermore, we have developed a g-

This work was supported in part by NSF (IIS 0916720, ECCS 1050236) and ONR (Grant N000140810640).

Feitian Zhang and X. Tan are with the Smart Microsystems Laboratory, Department of Electrical and Computer Engineering, Michigan State University, East Lansing, MI 48824, USA. Email: zhangzft@msu.edu (F. Z.), xbtan@egr.msu.edu (X. T.).

Fumin Zhang is with Electrical and Computer Engineering, Georgia Institute of Technology, Atlanta, GA 30332, USA. Email: fumin@gatech.edu (F. Z.).

Send correspondence to X. Tan. Tel: 1-517-432-5671; Fax: 1-517-353-1980.

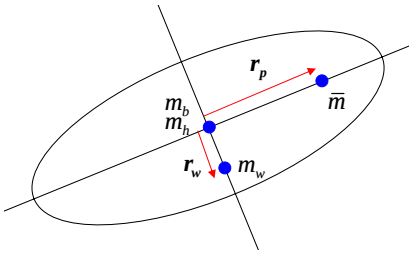


Fig. 1. The mass distribution of the gliding robotic fish (side view).

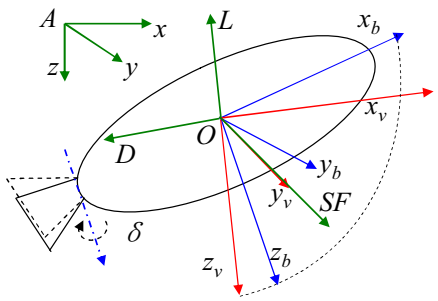


Fig. 2. Illustration of the reference frames and hydrodynamic forces for the gliding fish.

liding fish prototype, and performed experiments to compare the theoretical results with experimental observations.

## II. Dynamics Modeling of a Gliding Fish

### A. Full Dynamic Model

A gliding robotic fish is a combination of a miniature underwater glider and a robotic fish, and the modeling for a gliding robotic fish combines the models of both, mainly based on the model of an underwater glider, with the flapping tail treated as one of the sources for external forces and moments. In this paper, we model the gliding fish as a rigid body system, including one internal movable mass, whose location is controllable, like a miniature underwater glider, with an adjustable tank inside for tuning the net buoyancy [17], [18]. On the other hand, the flapping tail provides external thrust force and side force as well as the yaw moment as modeled in most robotic fish literature [10].

Fig. 1 shows mass distribution of the gliding fish system. The stationary body mass $m_s$ (excluding the movable mass) has three components: gliding fish hull mass $m_h$ (uniformly distributed), point mass $m_w$ for gliding fish nonuniform hull with displacement $\boldsymbol{r_w}$ with respect to the geometry center (GC), and ballast mass $m_b$ (water in the tank) at GC, which is a simplification since the effect on the center of gravity caused by the water in the tank is negligible compared with the moving mass. The movable mass $\bar{m}$, which is located at $\boldsymbol{r_p}$ with respect to GC, provides a torque to the gliding fish system. The mechanism for the moving mass is a track system fixed along the longitudinal axis inside the fish body and driven by a linear actuator. The fish body displaces a volume of fluid of mass $m$ . Let $m_0 = m_s + \bar{m} - m$ represents the excess mass (negative net buoyancy). The gliding fish will sink if $m_0 > 0$ and vice versa.

The relevant coordinate reference frames are defined following the standard convention. The body-fixed reference frame, denoted as $Ox_by_bz_b$ and shown in Fig. 2, has its origin $O$ at the geometry center, so the origin will be the point of application for the buoyancy force. The $Ox_b$ axis is along the body's longitudinal axis pointing to the head; the $Oz_b$ axis is perpendicular to $Ox_b$ axis in the sagittal plane of the gliding fish pointing downward, and $Oy_b$ axis is automatically formed by the right-hand orthonormal principle. In the inertial frame $Axyz$, $Az$ axis is along gravity direction, and $Ax$ is defined in the horizontal plane, while the origin $A$ is a fixed point in space.

As commonly used in the literature, $\boldsymbol{R}$ represents the rotation matrix from the body-fixed reference frame to the inertial frame. $\boldsymbol{R}$ is parameterized by three Euler angles: the roll angle $\phi$, the pitch angle $\theta$ and the yaw angle $\psi$. Let $\boldsymbol{v_b} = \begin{bmatrix} v_1 & v_2 & v_3 \end{bmatrix}^T$ and $\boldsymbol{\omega_b} = \begin{bmatrix} \omega_1 & \omega_2 & \omega_3 \end{bmatrix}^T$ stand for the translational velocity and angular velocity, respectively, expressed in the body-fixed frame. The subscript $b$ indicates that the vector is expressed in the body-fixed frame, and this notation is applied throughout this paper. Here

$$\boldsymbol{R} = \begin{pmatrix} c\theta c\phi & s\phi s\theta c\psi - c\phi s\psi & c\phi s\theta c\psi + s\phi s\psi \\ c\theta s\psi & c\phi c\psi + s\phi s\theta s\psi & -s\phi c\psi + c\phi s\theta s\psi \\ -s\theta & s\phi c\theta & c\phi c\theta \end{pmatrix} \tag{1}$$

where $s(\cdot)$ is short for $\sin(\cdot)$ and $c$ for $\cos(\cdot)$.

We assume the gliding fish tail is rigid and pivots at the junction of the fish body and the tail along $Oz_b$ direction. The tail induces an external thrust force $\boldsymbol{F_t}$ on the gliding fish body when the tail flaps. There are also hydrodynamic forces and moments, coming from the interaction between the tail and the relatively flowing water.

By incorporating the tail model into the existing derived dynamic model of underwater gliders [17], we get the following dynamics model for the gliding robotic fish:

$$\dot{\boldsymbol{v}}_{\boldsymbol{b}} = \boldsymbol{M}^{-1}\left(\boldsymbol{M}\boldsymbol{v_b} \times \boldsymbol{\omega_b} + m_0 g \boldsymbol{R}^{\boldsymbol{T}}\boldsymbol{k} + \boldsymbol{F_{ext}}\right) \tag{2}$$

$$\begin{aligned} \dot{\boldsymbol{\omega}}_{\boldsymbol{b}} = \boldsymbol{J}^{-1}\Big(&-\dot{\boldsymbol{J}}\boldsymbol{\omega_b} + \boldsymbol{J}\boldsymbol{\omega_b} \times \boldsymbol{\omega_b} + \boldsymbol{M}\boldsymbol{v}_b \times \boldsymbol{v_b} + \boldsymbol{T_{ext}} \\ &+ m_w g \boldsymbol{r_w} \times \left(\boldsymbol{R}^{\boldsymbol{T}}\boldsymbol{k}\right) + \bar{m} g \boldsymbol{r_p} \times \left(\boldsymbol{R}^{\boldsymbol{T}}\boldsymbol{k}\right)\Big) \end{aligned} \tag{3}$$

Here $\boldsymbol{M} = (m_s + \bar{m})\boldsymbol{I} + \boldsymbol{M_f}$, where $\boldsymbol{I}$ is the $3 \times 3$ identity matrix, and $\boldsymbol{M_f}$ is the added-mass matrix, which can be calculated via strip theory [19]. $\boldsymbol{J}$ is the sum of the inertia matrix due to the stationary mass distribution and the added inertia matrix in water. $\boldsymbol{k}$ is the unit vector along the $Az$ direction in the inertial frame. $\boldsymbol{r_w}$ is a constant vector, and $\boldsymbol{r_p}$ is the controllable movable mass position, which in our gliding fish design has one degree of freedom in $Ox_b$ direction, $\boldsymbol{r_p} = \begin{bmatrix} r_p & 0 & 0 \end{bmatrix}^T$. $\boldsymbol{F_{ext}}$ stands for all external forces: the external thrust force $\boldsymbol{F_t}$ induced by tail flapping, and the external hydrodynamic forces (lift force, drag force and side force) acting on the gliding fish body, expressed in the body-fixed frame. And $\boldsymbol{T_{ext}}$ is the total hydrodynamic moment caused by $\boldsymbol{F_{ext}}$.

$$
\begin{aligned}
0 &= m_2 s\beta V c\phi c\theta\omega_{3i} - m_3 s\alpha c\beta V s\phi c\theta\omega_{3i} - m_0 g s\theta - 1/2\rho V^2 S(C_{D0} + C_D^\alpha \alpha^2 + C_D^\delta \delta^2) c\alpha c\beta \\
&\quad -1/2\rho V^2 S(C_{SF}^\beta \beta + C_{SF}^\delta \delta) c\alpha s\beta + 1/2\rho V^2 S(C_{L0} + C_L^\alpha \alpha) s\alpha \qquad (21) \\
0 &= -m_3 s\alpha c\beta V s\theta\omega_{3i} - m_1 c\alpha c\beta V c\phi c\theta\omega_{3i} + m_0 g s\phi c\theta - 1/2\rho V^2 S(C_{D0} + C_D^\alpha \alpha^2 + C_D^\delta \delta^2) s\beta \\
&\quad +1/2\rho V^2 S(C_{SF}^\beta \beta + C_{SF}^\delta \delta) c\beta \qquad (22) \\
0 &= m_1 c\alpha c\beta V s\phi c\theta\omega_{3i} + m_2 s\beta V s\theta\omega_{3i} + m_0 g c\phi c\theta - 1/2\rho V^2 S(C_{D0} + C_D^\alpha \alpha^2 + C_D^\delta \delta^2) s\alpha c\beta \\
&\quad -1/2\rho V^2 S(C_{SF}^\beta \beta + C_{SF}^\delta \delta) s\alpha s\beta - 1/2\rho V^2 S(C_{L0} + C_L^\alpha \alpha) c\alpha \qquad (23) \\
0 &= (J_2 - J_3) s\phi c\theta c\phi c\theta\omega_{3i}^2 + (m_2 - m_3) s\beta s\alpha c\beta V^2 - m_w g r_w s\phi c\theta + 1/2\rho V^2 S(C_{M_R}^\beta \beta - K_{q1} s\theta\omega_{3i}) c\alpha c\beta \\
&\quad -1/2\rho V^2 S(C_{M_0} + C_{M_P}^\alpha \alpha + K_{q2} s\phi c\theta\omega_{3i}) c\alpha s\beta - 1/2\rho V^2 S(C_{M_Y}^\beta \beta + K_{q3} c\phi c\theta\omega_{3i} + C_{M_Y}^\delta \delta) s\alpha \qquad (24) \\
0 &= (J_1 - J_3) s\theta c\phi c\theta\omega_{3i}^2 + (m_3 - m_1) c\alpha c\beta s\alpha c\beta V^2 - m_w g r_w s\theta - \bar{m} g r_p c\phi c\theta \\
&\quad +1/2\rho V^2 S(C_{M_R}^\beta \beta - K_{q1} s\theta\omega_{3i}) s\beta + 1/2\rho V^2 S(C_{M_0} + C_{M_P}^\alpha \alpha + K_{q2} s\phi c\theta\omega_{3i}) c\beta \qquad (25) \\
0 &= (J_2 - J_1) s\theta s\phi c\theta\omega_{3i}^2 + (m_1 - m_2) c\alpha c\beta s\beta V^2 + \bar{m} g r_p s\phi c\theta + 1/2\rho V^2 S(C_{M_R}^\beta \beta - K_{q1} s\theta\omega_{3i}) s\alpha c\beta \\
&\quad -1/2\rho V^2 S(C_{M_0} + C_{M_P}^\alpha \alpha + K_{q2} s\phi c\theta\omega_{3i}) s\alpha s\beta + 1/2\rho V^2 S(C_{M_Y}^\beta \beta + K_{q3} c\phi c\theta\omega_{3i} + C_{M_Y}^\delta \delta) c\alpha \qquad (26)
\end{aligned}
$$

### B. Hydrodynamic Model

In order to model hydrodynamics, we first introduce the velocity reference frame $Ox_v y_v z_v$. $Ox_v$ axis is along the direction of velocity, and $Oz_v$ lies in the sagittal plane perpendicular to $Ox_v$. Rotation matrix $\boldsymbol{R_{bv}}$ represents the rotation operation from the velocity reference frame to the body-fixed frame:

$$
\boldsymbol{R_{bv}} = \begin{pmatrix} c\alpha c\beta & -c\alpha s\beta & -s\alpha \\ s\beta & c\beta & 0 \\ s\alpha c\beta & -s\alpha s\beta & c\alpha \end{pmatrix} \qquad (4)
$$

, where the angle of attack $\alpha = \arctan(v_3/v_1)$ and the sideslip angle $\beta = \arcsin(v_2/\|\boldsymbol{v_b}\|)$

The hydrodynamic forces include the lift force $L$, the drag force $D$, and the side force $SF$; hydrodynamic moments include the roll moment $M_1$, the pitch moment $M_2$, and the yaw moment $M_3$. All of those forces and moments are defined in the velocity frame [20]. And if we further assume the tail is not flapping, which means $\boldsymbol{F_t} = \boldsymbol{0}$, we will have the following relationship:

$$
\boldsymbol{F_{ext}} = \boldsymbol{R_{bv}} \begin{bmatrix} -D & SF & -L \end{bmatrix}^T \qquad (5)
$$

$$
\boldsymbol{T_{ext}} = \boldsymbol{R_{bv}} \begin{bmatrix} M_1 & M_2 & M_3 \end{bmatrix}^T \qquad (6)
$$

The hydrodynamic forces and moments are generally dependant on the angle of attack $\alpha$, the sideslip angle $\beta$, and the velocity magnitude $V$ [21], [22]:

$$
\begin{aligned}
D &= 1/2\rho V^2 S(C_{D0} + C_D^\alpha \alpha^2 + C_D^\delta \delta^2) \qquad (7) \\
SF &= 1/2\rho V^2 S(C_{SF}^\beta \beta + C_{SF}^\delta \delta) \qquad (8) \\
L &= 1/2\rho V^2 S(C_{L0} + C_L^\alpha \alpha) \qquad (9) \\
M_1 &= 1/2\rho V^2 S(C_{M_R}^\beta \beta + K_{q1}\omega_1) \qquad (10) \\
M_2 &= 1/2\rho V^2 S(C_{M_0} + C_{M_P}^\alpha \alpha + K_{q2}\omega_2) \qquad (11) \\
M_3 &= 1/2\rho V^2 S(C_{M_Y}^\beta \beta + K_{q3}\omega_3 + C_{M_Y}^\delta \delta) \qquad (12)
\end{aligned}
$$

where $\rho$ is the density of water and $S$ is the characteristic area of the gliding fish. $\delta$ is defined as the tail angle, the angle between the longitudinal axis and the center line of the tail projected into the $Ox_b y_b$ plane, with $Oz_b$ axis as the positive direction. $K_{q1}, K_{q2}, K_{q3}$ are rotation damping coefficients. All other constants with '$C$' in their notations are hydrodynamic coefficients, whose value can be evaluated through CFD-based water tunnel simulation as we did for the miniature glider [17] [23].

## III. Three-dimension Spiraling Motion of the Gliding Fish

We have three control variables available to manipulate the gliding fish swimming profile: excess mass $m_0$, the position of the movable mass $\boldsymbol{r_p}$ and the tail angle $\delta$. In this section, we analyze the steady-state spiraling equations with three control inputs fixed and use the Newton' method to solve the equations recursively.

### A. Steady-State Spiraling Equations

If control inputs are fixed with nonzero tail angle, we can treat the influence of the tail on the hydrodynamic forces and moments as the effects of increased hydrodynamic angles ($\alpha$, $\beta$). From [16], we know that the gliding fish will perform three-dimension steady spiraling motion, where the yaw angle $\psi$ changes at constant rate while the roll angle $\phi$ and pitch angle $\theta$ are constants. Then $\boldsymbol{R^T k}$ is constant since

$$
\boldsymbol{R^T k} = \boldsymbol{R^T} \begin{pmatrix} 0 \\ 0 \\ 1 \end{pmatrix} = \begin{pmatrix} -\sin\theta \\ \sin\phi\cos\theta \\ \cos\phi\cos\theta \end{pmatrix} \qquad (13)
$$

Take time derivative of $\boldsymbol{R^T k}$, we have

$$
\boldsymbol{\omega_b} \times (\boldsymbol{R^T k}) = 0 \qquad (14)
$$

, so the angular velocity has only one freedom with $\omega_{3i}$ in $Ox$ axis in the inertial frame. Then

$$
\boldsymbol{\omega}_b = \omega_{3i}(\boldsymbol{R^T k}) \qquad (15)
$$

$$\partial f_1/\partial x_1 = -m_2 s\beta V c\phi s\theta\omega_{3i} + m_3 s\alpha c\beta V s\phi s\theta\omega_{3i} - m_0 g c\theta \quad (30)$$

$$\partial f_1/\partial x_2 = -m_2 s\beta V s\phi c\theta\omega_{3i} - m_3 s\alpha c\beta V c\phi c\theta\omega_{3i} \quad (31)$$

$$\partial f_1/\partial x_3 = m_2 s\beta V c\phi c\theta - m_3 s\alpha c\beta V s\phi c\theta \quad (32)$$

$$\partial f_1/\partial x_4 = m_2 s\beta c\phi c\theta\omega_{3i} - m_3 s\alpha c\beta s\phi c\theta\omega_{3i} - m_0 g s\theta - \rho V S(C_{D0} + C_D^\alpha \alpha^2 + C_D^\delta \delta^2) c\alpha c\beta$$
$$-\rho V S(C_{SF}^\beta \beta + C_{SF}^\delta \delta) c\alpha s\beta + \rho V S(C_{L0} + C_L^\alpha \alpha) s\alpha \quad (33)$$

$$\partial f_1/\partial x_5 = -m_3 c\alpha c\beta V s\phi c\theta\omega_{3i} - \rho V^2 S C_D^\alpha \alpha c\alpha c\beta + 1/2\rho V^2 S(C_{D0} + C_D^\alpha \alpha^2 + C_D^\delta \delta^2) s\alpha c\beta$$
$$+1/2\rho V^2 S(C_{SF}^\beta \beta + C_{SF}^\delta \delta) s\alpha s\beta + 1/2\rho V^2 S C_L^\alpha s\alpha + 1/2\rho V^2 S(C_{L0} + C_L^\alpha \alpha) c\alpha \quad (34)$$

$$\partial f_1/\partial x_6 = m_2 c\beta V c\phi c\theta\omega_{3i} + m_3 s\alpha s\beta V s\phi c\theta\omega_{3i} + 1/2\rho V^2 S(C_{D0} + C_D^\alpha \alpha^2 + C_D^\delta \delta^2) c\alpha s\beta$$
$$-1/2\rho V^2 S C_{SF}^\beta c\alpha s\beta - 1/2\rho V^2 S(C_{SF}^\beta \beta + C_{SF}^\delta \delta) c\alpha c\beta \quad (35)$$

The translational velocity in the body-fixed frame

$$\boldsymbol{v_b} = \boldsymbol{R_{bv}} \begin{bmatrix} V & 0 & 0 \end{bmatrix}^T \quad (16)$$

There are two important parameters in the spiraling motion: the turning radius $R$ and the descending speed $V_{vertical}$. By projecting the total velocity into the horizontal plane and vertical direction, we have

$$R = V\cos(\theta - \alpha)/\omega_{3i} \quad (17)$$

$$V_{vertical} = V\sin(\theta - \alpha) \quad (18)$$

The steady-state spiraling equations are obtained by setting time derivatives to zero in (2), (3):

$$\mathbf{0} = \boldsymbol{M v_b} \times \boldsymbol{\omega_b} + m_0 g \boldsymbol{R^T k} + \boldsymbol{F_{ext}} \quad (19)$$

$$\mathbf{0} = \boldsymbol{J\omega_b} \times \boldsymbol{\omega_b} + \boldsymbol{M v_b} \times \boldsymbol{v_b} + \boldsymbol{T_{ext}} + m_w g \boldsymbol{r_w} \times \left(\boldsymbol{R^T k}\right) + \bar{m} g \boldsymbol{r_p} \times \left(\boldsymbol{R^T k}\right) \quad (20)$$

From equations (1), (4), (15), (16) and the above steady-state spiraling equations, we know there are six independent states for describing the steady spiral motion: $\begin{bmatrix} \theta & \phi & \omega_{3i} & V & \alpha & \beta \end{bmatrix}$ with $\begin{bmatrix} m_0 & r_p & \delta \end{bmatrix}$ as the three control inputs. Expanding equations (2) and (3), then transforming the original states to the above six independent states, we can obtain the nonlinear steady-state spiraling equations as in (21) - (26). Here, we assume the mass matrix and inertia matrix have the following form:

$$\boldsymbol{M} = \begin{pmatrix} m_1 & 0 & 0 \\ 0 & m_2 & 0 \\ 0 & 0 & m_3 \end{pmatrix} \quad \boldsymbol{J} = \begin{pmatrix} J_1 & 0 & 0 \\ 0 & J_2 & 0 \\ 0 & 0 & J_3 \end{pmatrix}$$

### *B. Newton's Method for Solving the Nonlinear Steady-State Spiraling Equations*

The steady-state spiraling equations are highly nonlinear due to the terms involving trigonometric functions and inverse trigonometric functions. Given the angle of attack, the sideslip angle, and the velocity magnitude, recursive algorithm for a fixed-point problem can be applied to solve the equations [16]. However, we are more interested in the steady-state solutions given fixed control inputs. Unfortunately, there is no feasible analytical solution and the convergence condition for the fixed-point problem is not satisfied either. So we use Newton's method to solve the spiraling steady states under fixed control inputs.

Let $\boldsymbol{x} = \begin{bmatrix} \theta & \phi & \omega_{3i} & V & \alpha & \beta \end{bmatrix}^T$ be the six states that we want to solve for steady-state spiral gliding equations. And let $\boldsymbol{u} = \begin{bmatrix} m_0 & r_p & \delta \end{bmatrix}^T$ be the three control inputs.

We write the governing equations in compact form here for convenience

$$0 = \boldsymbol{f}(\boldsymbol{x}, \boldsymbol{u}) = [f_i(\boldsymbol{x}, \boldsymbol{u})]_6 \quad (27)$$

Here, $f_i$ is the steady-state function of the spiraling motion. For example, $f_1$ is the right hand side of equation (21).

The iteration algorithm for Newton's method is [24]

$$\hat{\boldsymbol{x}}_{i+1} = \hat{\boldsymbol{x}}_i - J^{-1}(\hat{\boldsymbol{x}}_i, \boldsymbol{u}) \boldsymbol{f}(\hat{\boldsymbol{x}}_i, \boldsymbol{u}) \quad (28)$$

Here $\hat{\boldsymbol{x}}_i$ is the $i$th step estimation for the steady states, and $J(\boldsymbol{x}, \boldsymbol{u})$ is the Jocobian matrix of $f(\boldsymbol{x}, \boldsymbol{u})$

$$J(\boldsymbol{x}, \boldsymbol{u}) = \frac{\partial \boldsymbol{f}}{\partial \boldsymbol{x}} = \left[\frac{\partial f_i}{\partial x_j}\right]_{6\times 6} \quad (29)$$

Here, the first row elements of the Jocobian matrix are given in equations (30) - (35) while the others are omitted for succinct presentation, which can be calcluated simiarly.

## IV. Model prediction and Experimental Results on the Gliding Fish Prototype

We solve the steady-state spiraling equations using Newton's method for the lab-developed gliding fish prototype. Spiraling experiments with different control inputs are also conducted and the results are shown with good match between the model prediction and experimental results.

### *A. Solutions to the Steady-State Spiraling Equations for the Gliding Fish Prototype*

The spiraling motion is achieved using our fully untethered gliding fish prototype. This gliding fish prototype changes its net buoyancy by pumping water in and out of an inside tank, and varies its center of gravity via moving the battery pack using an linear actuator. Tails with different bending angles can be easily set up for the turning experiments. The prototype weighs 4 kg and measures 40 cm long with a 0.8 kg movable battery pack. Such a small size of the gliding fish, compared to traditional underwater gliders, renders it high

TABLE I

COMPUTED SPIRALING STEADY STATES THROUGH NEWTON'S METHOD.

| $m_0$ (g) | $r_p$ (cm) | $\delta(^\circ)$ | $(\theta, \phi, \omega_{3i}, V, \alpha, \beta)$ (°,°,rad/s,m/s,°,°) | $(V_{vertical}, R)$ (m/s,m) |
|---|---|---|---|---|
| 25 | 0.3 | 45 | (-44.5, -31.0, 0.425, 0.264, -0.914, 4.10) | (0.182, 0.450) |
| 25 | 0.4 | 45 | (-46.8, -36.6, 0.448, 0.267, -1.32, 4.52) | (0.190, 0.417) |
| 25 | 0.5 | 45 | (-48.3, -40.6, 0.464, 0.268, -1.61, 4.87) | (0.195, 0.396) |
| 25 | 0.6 | 45 | (-49.3, -43.8, 0.476, 0.267, -1.84, 5.18) | (0.197, 0.380) |
| 25 | 0.7 | 45 | (-50.2, -46.5, 0.486, 0.267, -2.04, 5.48) | (0.211, 0.338) |
| 10 | 0.5 | 45 | (-70.8, -49.3, 0.589, 0.184, -3.64, 7.36) | (0.169, 0.121) |
| 15 | 0.5 | 45 | (-63.5, -52.7, 0.571, 0.218, -3.30, 6.98) | (0.189, 0.190) |
| 20 | 0.5 | 45 | (-55.5, -47.8, 0.517, 0.247, -2.46, 5.85) | (0.197, 0.287) |
| 30 | 0.5 | 45 | (-42.1, -34.3, 0.423, 0.281, -0.901, 4.24) | (0.185, 0.500) |
| 35 | 0.5 | 45 | (-36.9, -29.3, 0.392, 0.289, -0.306, 3.85) | (0.172, 0.591) |
| 40 | 0.5 | 45 | (-32.3, -25.3, 0.368, 0.293, 0.224, 3.60) | (0.157, 0.670) |
| 25 | 0.5 | 30 | (-37.6, -11.9, 0.235, 0.242, 0.854, 2.19) | (0.151, 0.806) |
| 25 | 0.5 | 35 | ( -43.4, -20.7, 0.311, 0.258, 0.0698, 2.87) | (0.178, 0.602) |
| 25 | 0.5 | 40 | ( -46.8, -31.2, 0.389, 0.266, -0.761, 3.77) | (0.192, 0.474) |
| 25 | 0.5 | 50 | ( -49.2, -48.8, 0.537, 0.264, -2.54, 6.19) | (0.192, 0.337) |
| 25 | 0.5 | 55 | (-51.1, -56.4, 0.615, 0.257, -3.62, 7.86) | (0.190, 0.283) |
| 25 | 0.5 | 60 | ( -55.0, -63.8, 0.705, 0.247, -4.95, 10.0) | (0.189, 0.225) |

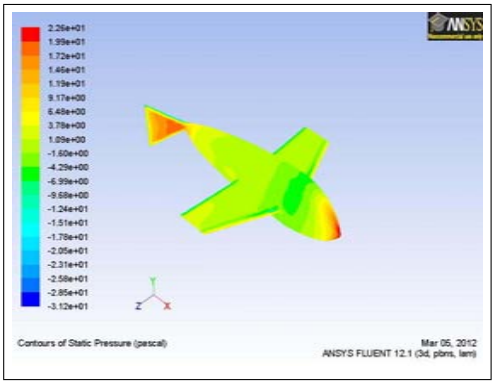


Fig. 3. Contours of the static pressure with tail angle at 45 °.

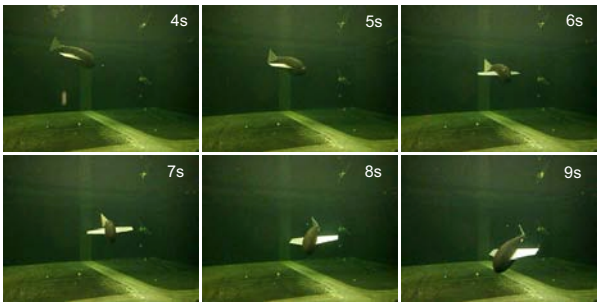


Fig. 4. Snap shots of gliding fish spiraling in the experiment tank.

maneuverability, like what it presents in spiraling motion in terms of turning radius. Hydrodynamic coefficients are determined by CFD simulation as in [17]. Here, we want to add that the hydrodynamic coefficients regarding the fish tail are obtained by curve fitting of the coefficients of different tail angles, which are evaluated by simulating the flow and pressure distribution using FLUENT6.2.16 in the CFD-based water channel experiments (Fig. 3).

Based on the parameters of this prototype, Newton's iterative formula (III-B) is used to solve the steady-state spiraling equations. Characteristic parameters for steady spiraling motion, including the turning radius and descending speed, are obtained with different inputs as shown in table I. To apply Newton's method, the initial values of states for iteration needs to be set rather than given any arbitrary values. However, for this spiraling equations, the selection is not strictly constrained. To get the table, we choose $\theta = -10^\circ, \phi = -10^\circ, \omega_{3i} = 0.1\text{rad/s}, \text{V} = 0.3\text{m/s}, \alpha = 0^\circ, \beta = 0^\circ$ as initial values for iteration, which leads to convergence. From the calculated results, we can see that a small turning radius requires a large tail angle, a large displacement of movable mass, and a small net buoyancy, while a low descending speed demands a small tail angle, a small displacement of movable mass, and a net buoyancy far away from 25 g. We utilize this relationship and conduct some experiments, selecting the control inputs to compensate the influence of the limitation of the experimental environment. The experimental results are presented in the next subsection.

### B. Experimental Results

With the lab-developed gliding fish prototype, underwater spiraling experiments are conducted in order to validate the derived mathematical models and Newton's recursive algorithm. Most experiments are conducted in a large water tank that measures 15-foot long, 10-foot wide, and 4-foot deep, as shown in Fig. 4. We set the net buoyancy (negatively buoyant), the linear actuator position and gliding fish tail angle to fixed values. Then the glider is released on the water surface and glides into spiraling mode. Cameras are set to record the videos in both top view and side view. The turning radius are extracted after video processing. The comparison between model predictions and experiment results on turning radius for different tail angles and different excess mass are shown in Fig. 5 and Fig. 6, respectively.

There are some factors contributing to the measurement errors. First, for different depth, the scales between real objects and camera image are different. Here, the average scale is used in the video processing. A grid board is used for calibration, captured with the same camera at the mean

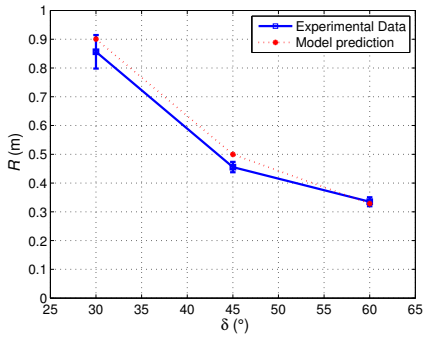


Fig. 5. Spiraling radius with respect to the tail angle, with fixed movable mass displacement of 0.5 cm and fixed excess mass of 30 g.

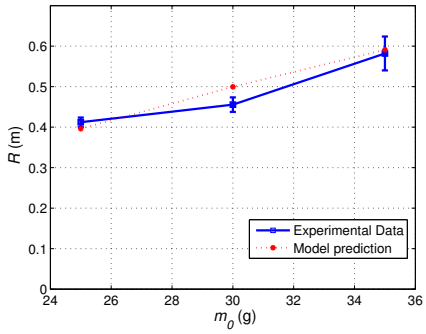


Fig. 6. Spiraling radius with respect to the excess mass , with fixed movable mass displacement of 0.5 cm and fixed tail angle of 45°.

distance. Second, although the transient is fast from stationary status to steady gliding motion due to the damping effect from the water, there is still some initial transient process, difficult to completely separate from the steady spiraling period. Experimental environment with deeper water will effectively reduce the influence of initial transient, however, the complexity of experiments setup will be increased as a result. The environmental disturbances such as currents will also affect the experimental results. So with these uncertainties, we consider the match between our experimental results and the model predictions satisfactory.

## V. CONCLUSION

In this paper we investigated a novel spiral motion for a gliding robotic fish, achieved by gliding with a deflected tail. Such spirals hold strong promise in water column sampling. Dynamic model of gliding fish was presented and steady-state spiraling equations were derived and analyzed. Newton's method was used to solve the equations. A gliding fish prototype was presented, and experiments were carried out to validate both the mathematical model and the recursive algorithm. In future work, we will analyze the basins of attraction for Newton's method, and instrument the gliding fish with environmental sensors for a field experiment.

## ACKNOWLEDGMENT

The authors would like to thank John Thon for his help in the development of the gliding fish prototype.

## REFERENCES

[1] C. C. Eriksen, T. J. Osse, R. Light, R. D. Wen, T. W. Lehmann, P. L. Sabin, J. W. Ballard, and A. M. Chiodi, "Seaglider: A long-range autonomous underwater vehicle for oceanographic research," *IEEE Journal of Oceanic Engineering*, vol. 26, no. 4, pp. 424–436, 2001.

[2] J. Sherman, R. E. Davis, W. B. Owens, and J. Valdes, "The autonomous underwater glider 'Spray'," *IEEE Journal of Oceanic Engineering*, vol. 26, no. 4, pp. 437–446, 2001.

[3] D. C. Webb, P. J. Simonetti, and C. P. Jones, "Slocum: An underwater glider propelled by environmental energy," *IEEE Journal of Oceanic Engineering*, vol. 26, no. 4, pp. 447–452, 2001.

[4] N. Kato, "Control performance in the horizontal plane of a fish robot with mechanical pectoral fins," *IEEE Journal of Oceanic Engineering*, vol. 25, no. 1, pp. 121–129, 2000.

[5] K. H. Low, "Locomotion and depth control of robotic fish with modular undulating fins," *International Journal of Automation and Computing*, vol. 4, pp. 348–357, 2006.

[6] M. S. Triantafyllou and G. S. Triantafyllou, "An efficient swimming machine," *Scientific America*, vol. 273, no. 3, pp. 64–70, 1995.

[7] J. Yu and L. Wang, "Parameter optimization of simplified propulsive model for biomimetic robot fish," in *Proceedings of the 2005 IEEE International Conference on Robotics and Automation*, Barcelona, Spain, 2005, pp. 3306–3311.

[8] H. Hu, J. Liu, I. Dukes, and G. Francis, "Design of 3d swim patterns for autonomous robotic fish," in *Proceedings of the 2006 IEEE/RSJ International Conference on Intelligent Robots and Systems*, Beijing, China, 2006, pp. 2406–2411.

[9] K. A. Morgansen, B. I. Triplett, and D. J. Klein, "Geometric methods for modeling and control of free-swimming fin-actuated underwater vehicles," *IEEE Transactions on Robotics*, vol. 23, no. 6, pp. 1184–1199, 2007.

[10] Z. C. S. Shatara and X. Tan, "Modeling of biomimetic robotic fish propelled by an ionic polymer-metal composite caudal fin," *IEEE/ASME Transactions on Mechatronics*, vol. 15, no. 3, pp. 448–459, 2010.

[11] X. Tan, "Autonomous robotic fish as mobile sensor platforms: Challenges and potential solutions," *Marine Technology Society Journal*, vol. 45, no. 4, pp. 31–40, 2011.

[12] M. Schwartz, *Encyclopedia of coastal science*. Kluwer Academic Pub, 2005, vol. 24.

[13] J. G. Graver, "Underwater gliders: Dynamics, control, and design," Ph.D. dissertation, Princeton University, 2005.

[14] P. Bhatta, "Nonlinear stability and control of gliding vehicles," Ph.D. dissertation, Princeton University, 2006.

[15] N. Mahmoudian, "Efficient motion planning and control for underwater gliders," Ph.D. dissertation, Virginia Polytechnic Institute and State University, 2009.

[16] S. Zhang, J. Yu, A. Zhang, and F. Zhang, "Steady three dimensional gliding motion of an underwater glider," in *2011 IEEE International Conference on Robotics and Automation (ICRA)*. IEEE, 2011, pp. 2392–2397.

[17] F. Zhang, J. Thon, C. Thon, and X. Tan, "Miniature underwater glider: Design, modeling, and experimental results," in *Proceedings of the 2012 IEEE International Conference on Robotics and Automation*, St. Paul, MN, 2012, pp. 4904–4910.

[18] N. E. Leonard and J. G. Graver, "Model-based feedback control of autonomous underwater gliders," *IEEE Journal of Oceanic Engineering*, vol. 26, no. 4, pp. 633–645, 2001.

[19] J. Milgram, "Strip theory for underwater vehicles in water of finite depth," *Journal of Engineering Mathematics*, vol. 58, no. 1, pp. 31–50, 2007.

[20] R. L. Panton, *Incompressible Flow*. New York: Wiley, 2005.

[21] D. T. Greenwood, *Principles of Dynamics*. Englewood Cliffs, NJ.: Prentice Hall, 1988.

[22] J. D. Anderson, *Aircraft Performance and Design*. New York: McGraw-Hill, 1998.

[23] D. Seo, G. Jo, and H. Choi, "Pitching control simulations of an underwater glider using CFD analysis," in *OCEANS 2008-MTS/IEEE Kobe Techno-Ocean*. IEEE, 2008, pp. 1–5.

[24] C. Kelley, *Solving nonlinear equations with Newton's method*. Society for Industrial Mathematics, 2003.